Journal of Materials Chemistry

Cite this: J. Mater. Chem., 2012, 22, 21502

www.rsc.org/materials

PAPER

Simultaneous enhancement of the carrier mobility and luminous efficiency through thermal annealing a molecular glass material and device

Shanfeng Xue,[a] Liang Yao,[a] Suijun Liu,[a] Cheng Gu,[a] Fangzhong Shen,[a] Weijun Li,[a] Hui Zheng,[a] Hongbin Wu[b] and Yuguang Ma*[a]

Received 16th July 2012, Accepted 31st August 2012
DOI: 10.1039/c2jm34663j

The molecule 2,5,2′,5′-tetrakis(2,2-diphenylvinyl)biphenyl (**TDPVBi**) shows excellent solubility in organic solvents, a fully amorphous (glass state) property and strong blue emission in the solid state, endowing it with potential to fabricate solution-processed small-molecular devices. To further improve the quality of **TDPVBi** films, thermal annealing of method was performed for the pristine films, as prepared from solution, and proved to be an efficient way to repair the defects (*e.g.* pinhole) that exist in the pristine films. It is found that the films tend to become compact with level surface morphology after thermal annealing at a temperature around their glass transition temperature (T_g). The device characteristics show that thermal annealing induces a simultaneous enhancement of the hole mobility and luminous efficiency. The luminous efficiency reaches 4.60 cd A^{-1} (corresponding external quantum efficiency of ~3.0%) after thermal annealing at a temperature of 120 °C, which is double that of the device without annealing.

Introduction

Since the pioneering discovery of organic light-emitting diodes (OLEDs) in 1987,[1] OLEDs have become an emerging technology for lighting and display, which have come to the commercial stage. Despite the great progress in OLED technology, there are still many opportunities to improve this technology (especially lowering cost) from both materials and devices aspects.[2–8] Recently, solution-processed small-molecule OLEDs (SMOLEDs) have aroused great interest in the organic optoelectronic community because of the low cost due to the solution-processing technique and the high performance due to the well-defined and contrivable structure and high purity of small molecules. Hereby, many works have been reported and have made great progress.[9–15] Generally, the small-molecule materials for solution-processed devices require some basic features, *e.g.* high solubility and glass state, particularity for high quality films, and high photoluminescence (PL) quantum efficiency and charge transporting ability for device operation. There have been case studies of high-performance spin-coated devices from small molecules and prototype display screens developed from ink-jet small molecules.[16,17]

With respect to most luminescent molecules designed for vacuum deposition, they are not typically suitable for the solution process. Firstly, the low solution viscosity of these small molecules is the major obstacle to obtaining high-quality and free-pinhole films from the solution spin-coating process. Unlike polymeric materials, whose polymer chains are extended in dilute solutions and shrink and then entangle with each other as the solvent dries out gradually, the structural adaptability of a small molecule to its environment (*e.g.* solvent evaporating) is relatively weak compared to polymer materials. This makes it difficult to form uniform and compact films from solution. Secondly, for small molecules, most of them are easy to crystallize, which will result in local aggregation to form pinholes during the solution spin-coating process. A principle issue for solution-processed small-molecule devices is the choice of materials with amorphous state in nature, which can avoid crystallization. At present, many works have been reported to improve the film quality of solution-processed small-molecule materials through molecular structure design, such as dendritic molecules,[18–20] oligomers[21–23] and starbursts.[24–26] Meanwhile, some physical methods have been used to make the films quality better,[27,28] typically using mixed solvents and blended small molecular materials. However, it is still difficult to obtain a pristine film without defects completely. In this work, the method of thermal annealing was used in solution-processed SMOLEDs and proved to be useful to repair the defects (*e.g.* pinhole) that exist in the pristine films, especially for the glass state small molecule materials. The results show that a thermal annealing method could enhance the carrier mobility and luminous efficiency simultaneously.

[a]*State Key Lab of Supramolecular Structure and Materials, Jilin University, 2699 Qianjin Avenue, Changchun, 130012, P. R. China. E-mail: ygma@jlu.edu.cn; Fax: +86 431-85168480; Tel: +86 431-85168480*
[b]*State Key Laboratory of Luminescent Materials and Devices, Institute of Polymer Optoelectronic Materials and Devices, South China University of Technology, Guangzhou 510640, P. R. China*

Results and discussion

The blue fluorescent molecule 2,5,2′,5′-tetrakis(2,2-diphenylvinyl)biphenyl (**TDPVBi**)[29] possesses the basic characteristics of solution-processed small-molecule materials, such as (1) high solubility, *c.a.* 20 mg mL^{-1} in THF, (2) fully glass-like morphology in the solid with a glass transition temperature (T_g) of 110 °C and (3) high PL quantum efficiency in the solid state, *c.a.* 0.80. Thus, it provided the basic earmarks for solution-processed fluorescent small-molecule OLEDs. Indeed, quite a smooth film can be formed by spin-coating from its THF solution. The atomic force microscopy (AFM) image shown in Fig. 1(b) exhibits a surface roughness (root mean square) (RMS) of 0.35 nm, which is suitable for device fabrication.

The device from the pristine **TDPVBi** films showed bright blue emission with good vidicon uniformity. The luminous efficiency is up to 2.24 cd A^{-1} at current density of 4.96 mA cm^{-2}. In order to improve the device performances, the thermal annealing treatments for pristine films were performed at 90 °C and 120 °C around T_g of **TDPVBi** in a nitrogen atmosphere dry-box for 20 minutes. Fig. 2 shows (a) the luminous efficiency–current density (LE–*J*) and (b) the current density–luminance–voltage (*J*–*L*–*V*) characteristics of these devices. Detailed data are listed in Table 1. The distinct effect of the thermal annealing process on the device performances was investigated. As the annealing temperature increased from room temperature (R. T.) to 120 °C, the efficiency of the devices increases greatly; 4.13 cd A^{-1} at annealing temperature 90 °C and 4.60 cd A^{-1} at annealing temperature 120 °C, respectively. The current density–luminance–voltage (*J*–*L*–*V*) (Fig. 2(b)) shows that the thermal annealing device has a turn-on voltage of 3.75 V, lower than that of the un-annealing one (4.25 V), and the current density is also superior to the un-annealing one, which indicated the more efficient carrier injection into the emitting-layer of the thermal annealing device. Thus, a more balanced hole and electron injection is expected and responsible for the improved device performance when using the thermal annealing method for emitting-layer films.

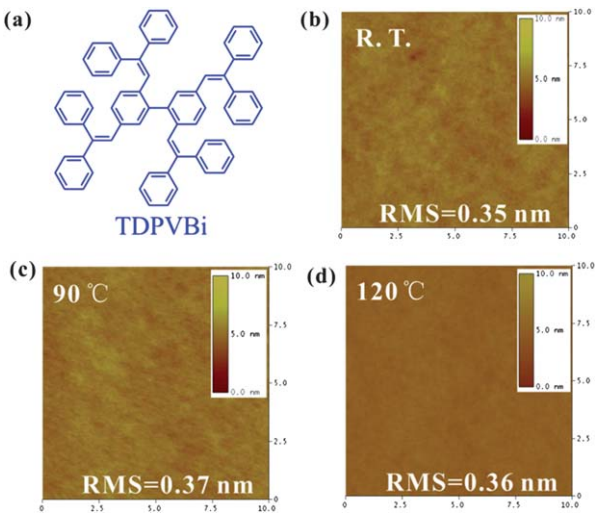

Fig. 1 (a) The chemical structure of **TDPVBi** and the AFM images of spin-coated films at different annealing temperatures: (b) room temperature (R. T.), (c) 90 °C, (d) 120 °C.

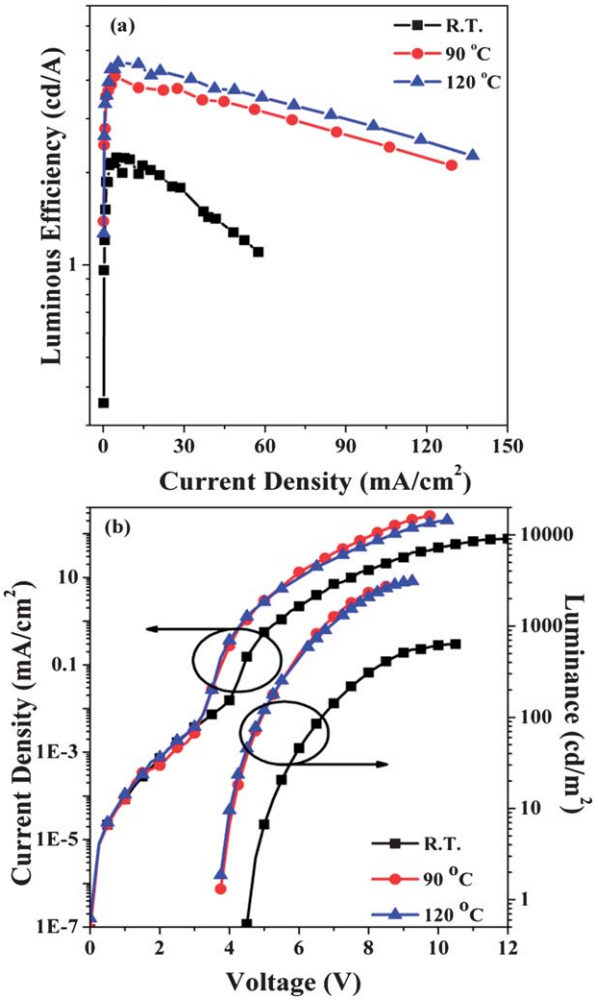

Fig. 2 (a) The luminous efficiency–current density (LE–*J*) and (b) the current density–luminance–voltage (*J*–*L*–*V*) characteristics of **TDPVBi** devices (ITO/PEDOT:PSS (40 nm)/**TDPVBi**/**TPBi** (40 nm)/CsF (1.5 nm)/Al (120 nm)) at different annealing temperatures.

The surface morphology of the films before and after thermal annealing were investigated by AFM and the results indicated that the annealing process has no clear effects on the surface morphology, *e.g.* the RMS of un-annealing **TDPVBi** films is 0.35 nm (Fig. 1(b)), and the RMS are 0.37 nm (Fig. 1(c)) and 0.36 nm (Fig. 1(d)) after annealing at 90 °C and 120 °C, respectively. But the thickness of **TDPVBi** films, which is measured by the surface profiler is found to reduce by 10 nm (from ~85 nm to ~75 nm) after annealing with a ~10% reduction of thickness relative to pristine films. This indicates the formation of more compact films after annealing, which may be beneficial for the carrier injection and transporting in the device.

Fig. 3 shows the current density–voltage (*J*–*V*) characteristics of the hole-only device with the structure of ITO/PEDOT:PSS (40 nm)/**TDPVBi**/MoO_3 (10 nm)/Al (80 nm). It was found that the hole current density of films annealing at 120 °C was the highest in all films involving pristine films and annealing films below a T_g of 110 °C. It suggests the possibility that increasing hole current density leads to a higher performance of devices. In other words, the electron and the hole become more balanced with device annealing at 120 °C.

Table 1 The performances of devices under the different treatment conditions

	The maximums of quantum efficiency							
Treatment conditions	Voltage (V)	J (mA cm^{-2})	L (cd m^{-2})	LE_{max}[a] (cd A)	QE_{max}[b] (%)	L_{max}[c] (cd m^{-2})	$V_{turn\text{-}on}$[d] (V)	CIE (x, y)[e]
R.T.	6.75	4.96	111	2.24	1.47	634	4.50	0.21, 0.32
90 °C	5.25	4.29	177	4.13	2.71	2767	3.75	0.20, 0.31
120 °C	5.50	5.54	252	4.60	2.98	3106	3.75	0.20, 0.32

[a] Maximal front viewing luminous efficiency in cd A^{-1}. [b] Maximal external quantum efficiency in %. [c] Maximum luminance. [d] Defined as the bias voltage at the luminance of 1 cd m^{-2}. [e] Observer: 2°; obtained at 10 mA cm^{-2}.

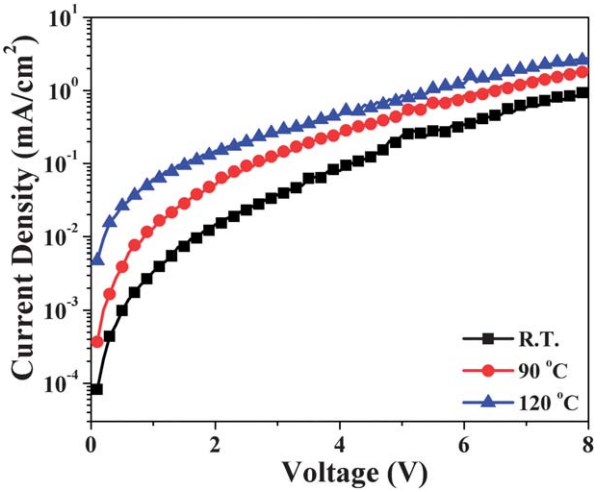

Fig. 3 The current density–voltage (J–V) characteristics of the hole-only devices (ITO/PEDOT:PSS (40 nm)/**TDPVBi**/MoO_3 (10 nm)/Al (80 nm)) at different annealing temperatures.

Fig. 4 shows the electroluminescence (EL) spectra after thermal annealing. As can be seen, the spectra have nearly no differences compared to that of pristine films. These phenomena reflect that no obvious structure change in the condensed state after the annealing at temperatures even up to 120 °C. This may be related to the glass state nature of **TDPVBi** molecules, which suppresses the strong intermolecular interactions, such as molecular crystalline and π–π interactions.

From the energy level diagram of the **TDPVBi** device (Fig. 5), the carriers combination and emitting zone should be localized at the interface of **TDPVBi/TPBi** because of the role of the **TPBi** layer in electron injection and hole blocking. The barrier for holes is estimated from the HOMO level of **TDPVBi** and **TPBi** to be 0.7 eV. This means that the holes, which pass over the **TDPVBi** layer, can be obstructed on the interface of **TDPVBi/TPBi** effectively. Because the electron injection from the **TPBi** layer is very efficient, the majority of electrons should be in the interface zone. Thus, if more holes can arrive and be cumulated at this interface, it should be beneficial to their recombination with injecting electrons. This may be the reason for the great enhancement of device efficiency after thermal annealing, which can improve the hole mobility and thus transport more hole carriers to the recombination interface.

The origin of thermal annealing for **TDPVBi** and its effect on carrier transport and luminous efficiency should be relative to the structural speciality of the **TDPVBi** molecule. The **TDPVBi** is a cruciform compound, in which two 4,4′-bis(2,2-diphenylvinyl)-1,1′-biphenyl (DPVBi)[30–32] segments are linked through a central biphenyl linkage. In a pristine film, the spatial hindrance between the arms of the cruciform structure may prevent the **TDPVBi** molecules from packing closely, as films form from solvent evaporating rapidly, which make the films less compact and exist in a large free-volume. The biphenyl core in such cruciform structures has an ability of free rotation as the environment

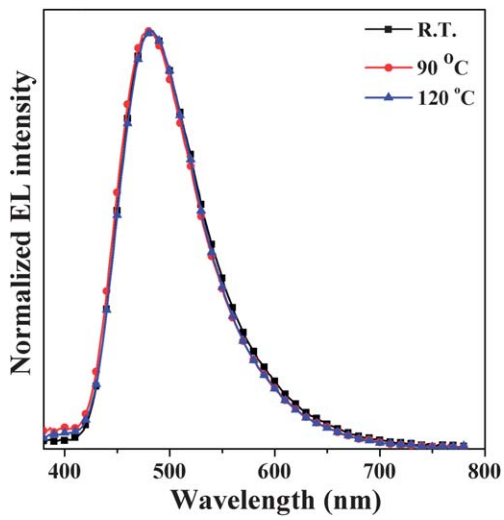

Fig. 4 The EL spectra of devices at different thermal annealing temperatures.

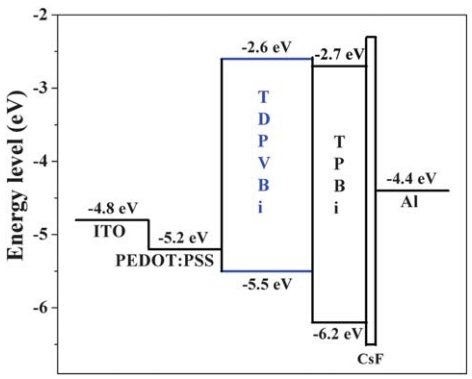

Fig. 5 The energy level diagram of the **TDPVBi** device (ITO/PEDOT:PSS (40 nm)/**TDPVBi/TPBi** (40 nm)/CsF (1.5 nm)/Al (120 nm)).

temperature is elevated to its T_g, providing the molecule with proper flexibility. At the thermal annealing temperature over its T_g (120 °C), rotational motion around the biphenyl core induces a reorganization of molecules in films and in the present observed case the effect is to make the films become more dense. More compact films after thermal annealing should correspond to enhanced hole current density, which is observed from the measurement of the single carrier devices. In general, tight molecular packing does not help to realize the high fluorescence in the solid state. But the fluorescence investigations demonstrate the**TDPVBi** molecule with a positive effect as molecule aggregation. The fluorescence of **TDPVBi** in solution is barely detectable, but their solid films show a brilliant blue fluorescence when excited using a UV lamp, which indicates **TDPVBi** to be a typical material of aggregation-induced emission (AIE).[33–35] According to the understanding of AIE phenomena, the AIE property of the **TDPVBi** molecule should be relative to its free rotation of end phenyl groups in solution (fluorescence quenching) and restrained free rotation of end phenyl groups in the solid state because of intermolecular interactions.[29] Accordingly, more compact molecular packing and less free volume in the thermal annealing film is beneficial to high fluorescence of such an AIE molecule.

Experimental

Materials

TDPVBi was synthesized in our laboratory as previously reported.[29] 1,3,5-tri(phenyl-2-benzimidazolyl)-benzene (**TPBi**) and caesium fluoride (CsF) were purchased commercially and used as an electron-injection layer and interface modification layer, respectively. They were used without purifying. The chemical structure of **TDPVBi** is shown in Fig. 1(a).

Instruments

SMOLEDs based on **TDPVBi** were prepared with a structure of indium-tin oxide (ITO)/poly(3,4-polyethlenedioxythiophene)-polystyrenesulfonate (PEDOT:PSS) (40 nm)/**TDPVBi/TPBi** (40 nm)/CsF (1.5 nm)/Al (120 nm). Indium-tin oxide (ITO) coated glass with a sheet resistance of 15–20 Ω square^{-1} was cleaned using the standard procedure and then dried in an oven. After oxygen plasma cleaning for 4 min, a 40 nm-thick poly(3,4-ethylenedioxythiopene):poly(styrenesulfonate) (PEDOT:PSS) (Bayer Baytron 4083) layer was first spin-coated onto the ITO substrate from water solution and then dried by baking in a vacuum oven at 80 °C overnight. Then, the emissive layer **TDPVBi** was spin-coated on the PEDOT:PSS layer from THF solution. The emissive layer **TDPVBi** with thermal annealing was performed at 90 °C and 120 °C around T_g in a nitrogen atmosphere dry-box for 20 minutes. The thicknesses of these organic films were determined by the surface profiler (Tencor Alfa-Step 500). Next, 1,3,5-tris(1-phenyl-1*H*-benzo[*d*]imidazol-2-yl) benzene (**TPBi**) acted as an electron injection and hole block layer, which was thermally deposited onto the **TDPVBi**-layer under a vacuum at a pressure of 3×10^{-4} Pa. At last, the CsF/Al cathode was thermally deposited onto the **TPBi**-layer under a vacuum at a pressure of 3×10^{-4} Pa. The substrate was prepatterned by photolithography to give an effective device size of 19 mm^2. The current density–luminance–voltage (*J–L–V*) characteristics were measured by a Keithley 236 source measurement unit. The electroluminescent (EL) spectra were measured using a PR-705 Spectroscan spectrometer. The device fabrication, except PEDOT:PSS coating, was carried out in a nitrogen atmosphere dry-box (Vacuum Atmosphere Co.) containing less than 10 ppm oxygen and moisture. The atomic force microscopy (AFM) image was recorded on a Seiko SPA 400 with an SPI 3800 probe station in tapping mode (dynamic force mode).

Conclusions

In summary, we demonstrate that the quality of the solution-processed films of **TDPVBi** with glass state property could be promoted by thermal annealing. Thermal annealing was found to be an efficient method to make the films more compact, enhance the hole carrier mobility and improve the device luminous efficiency by approximately twice compared to the un-annealing device. The study provide a promising approach to repair the defects of pristine films in solution-processed SMOLEDs and enhance the device performances, especially for the AIE molecule with glass state property.

Acknowledgements

This work was supported by grants from the Natural Science Foundation of China (20834006, 20872047), the Ministry of Science and Technology of China (2009CB623605), 111 project (B06009) and PCSIRT.

References

1 C. W. Tang and S. A. VanSlyke, *Appl. Phys. Lett.*, 1987, **51**, 913–915.
2 Z. Y. Ge, T. Hayakawa, S. Ando, M. Ueda, T. Akiike, H. Miyamoto, T. Kajita and M. Kakimoto, *Chem. Mater.*, 2008, **20**, 2532–2537.
3 L. Wang, Y. Jiang, J. Luo, Y. Zhou, J. H. Zhou, J. Wang, J. Pei and Y. Cao, *Adv. Mater.*, 2009, **21**, 4854–4858.
4 Y. Zhou, Q. G. He, Y. Yang, H. Z. Zhong, C. He, G. Y. Sang, W. Liu, C. H. Yang, F. L. Bai and Y. F. Li, *Adv. Funct. Mater.*, 2008, **18**, 3299–3306.
5 S. F. Xue, L. Yao, F. Z. Shen, C. Gu, H. B. Wu and Y. G. Ma, *Adv. Funct. Mater.*, 2012, **22**, 1092–1097.
6 S. A. Van Slyke, C. H. Chen and C. W. Tang, *Appl. Phys. Lett.*, 1996, **69**, 2160–2162.
7 S. A. Carter, J. C. Scott and P. J. Brock, *Appl. Phys. Lett.*, 1997, **71**, 1145–1147.
8 L. S. Hung and C. W. Tang, *Appl. Phys. Lett.*, 1999, **74**, 3209–3211.
9 M. Zhang, S. F. Xue, W. Y. Dong, Q. Wang, T. Fei, C. Gu and Y. G. Ma, *Chem. Commun.*, 2010, **46**, 3923–3925.
10 L. Yao, S. F. Xue, Q. Wang, W. Y. Dong, W. Yang, H. B. Wu, M. Zhang, B. Yang and Y. G. Ma, *Chem.–Eur. J.*, 2012, **18**, 2707–2714.
11 J. Huang, Q. Liu, J. H. Zou, X. H. Zhu, A. Y. Li, J. W. Li, S. Wu, J. B. Peng, Y. Cao, R. D. Xia, D. D. C. Bradley and J. Roncali, *Adv. Funct. Mater.*, 2009, **19**, 2978–2986.
12 A. L. Fisher, K. E. Linton, K. T. Kamtekar, C. Pearson, M. R. Bryce, M. C. Petty and M. C. Petty, *Chem. Mater.*, 2011, **23**, 1640–1642.
13 L. Duan, L. D. Hou, T. W. Lee, J. Qiao, D. Q. Zhang, G. F. Dong, L. D. Wang and Y. Qiu, *J. Mater. Chem.*, 2010, **20**, 6392–6407.
14 T. S. Qin, G. Zhou, H. Scheiber, R. E. Bauer, M. Baumgarten, C. E. Anson, E. J. W. List and K. Müllen, *Angew. Chem., Int. Ed.*, 2008, **47**, 8292–8296.
15 H. Huang, Q. Fu, S. Q. Zhuang, G. Y. Mu, L. Wang, J. S. Chen, D. G. Ma and C. L. Yang, *Org. Electron.*, 2011, **12**, 1716–1723.

16 B. J. Gans, P. C. Duineveld and U. S. Schubert, *Adv. Mater.*, 2004, **16**, 203–213.
17 C. R. McNeill and N. C. Greenham, *Adv. Mater.*, 2009, **21**, 3840–3850.
18 Z. A. Li, Z. Q. Jiang, S. H. Ye, C. K. W. Jim, G. Yu, Y. Q. Liu, J. G. Qin, B. Z. Tang and Z. Li, *J. Mater. Chem.*, 2011, **21**, 14663–14671.
19 J. Y. Li and D. Liu, *J. Mater. Chem.*, 2009, **19**, 7584–7591.
20 S. K. Hwang, C. N. Moorefield and G. R. Newkome, *Chem. Soc. Rev.*, 2008, **37**, 2543–2557.
21 Q. Q. Li, J. H. Zou, J. W. Chen, Z. J. Liu, J. G. Qin, Z. Li and Y. Cao, *J. Phys. Chem. B*, 2009, **113**, 5816–5822.
22 T. Matsushima and C. Adachi, *Chem. Mater.*, 2008, **20**, 2881–2883.
23 Y. H. Geng, S. W. Culligan, A. Trajkovska, J. U. Wallace and S. H. Chen, *Chem. Mater.*, 2003, **15**, 542–549.
24 C. Liu, Y. H. Li, Y. Y. Zhang, C. L. Yang, H. B. Wu, J. G. Qin and Y. Cao, *Chem.–Eur. J.*, 2012, **18**, 6928–6934.
25 J. Pei, J. L. Wang, X. Y. Cao, X. H. Zhou and W. B. Zhang, *J. Am. Chem. Soc.*, 2003, **125**, 9944–9945.
26 A. L. Kanibolotsky, R. Berridge, P. J. Skabara, I. F. Perepichka, D. D. C. Bradley and M. Koeberg, *J. Am. Chem. Soc.*, 2004, **126**, 13695–13702.
27 T. W. Lee, T. Noh, H. W. Shin, O. Kwon, J. J. Park, B. K. Choi, M. S. Kim, D. W. Shin and Y. R. Kim, *Adv. Funct. Mater.*, 2009, **19**, 1625–1630.
28 D. D. Wang, Z. X. Wu, X. W. Zhang, B. Jiao, S. X. Liang, D. W. Wang, R. L. He and X. Hou, *Org. Electron.*, 2010, **11**, 641–648.
29 S. J. Liu, F. He, H. Wang, H. Xu, C. Y. Wang, F. Li and Y. G. Ma, *J. Mater. Chem.*, 2008, **18**, 4802–4807.
30 C. Hosokawa, H. Tokailin, H. Higashi and T. Kusumoto, *Appl. Phys. Lett.*, 1993, **63**, 1322–1324.
31 C. Hosokawa, H. Tokailin, H. Higashi and T. Kusumoto, *J. Appl. Phys.*, 1995, **78**, 5831–5833.
32 C. Hosokawa, H. Higashi, H. Nakamura and T. Kusumoto, *Appl. Phys. Lett.*, 1995, **67**, 3853–3855.
33 Z. J. Zhao, S. M. Chen, C. M. Deng, J. W. Y. Lam, C. Y. K. Chan, P. Lu, Z. M. Wang, B. B. Hu, X. P. Chen, P. Lu, H. S. Kwok, Y. G. Ma, H. Y. Qiu and B. Z. Tang, *J. Mater. Chem.*, 2011, **21**, 10949–10956.
34 Y. N. Hong, J. W. Y. Lam and B. Z. Tang, *Chem. Soc. Rev.*, 2011, **40**, 5361–5388.
35 Y. P. Li, F. Li, H. Y. Zhang, Z. Q. Xie, W. J. Xie, H. Xu, B. Li, F. Z. Shen, L. Ye, M. Hanif, D. G. Ma and Y. G. Ma, *Chem. Commun.*, 2007, 231–233.

